JACS
JOURNAL OF THE AMERICAN CHEMICAL SOCIETY

ARTICLE

pubs.acs.org/JACS

Reactivity Trends within Alkoxy Radical Reactions Responsible for Chain Branching

Alexander C. Davis* and Joseph S. Francisco*

Department of Chemistry and Department of Earth and Atmospheric Science, Purdue University, West Lafayette, Indiana 47907-1393, United States

Supporting Information

ABSTRACT: Alkoxy radicals are a key component in both the atmospheric and combustion oxidation pathways of traditional and alternative fuels. An accurate description of their chemistry as it alters with reaction conditions is essential to understanding atmospheric and combustion processes involving hydrocarbons. Experimental and theoretical data on alkoxy radicals and their reactions are scarce, especially for larger chain systems and high temperatures. The present work investigates all unimolecular reactions of the methoxy through heptoxy radicals using the CBS-Q, G2, and G4 composite computational methods. After analysis of the resulting thermodynamic and kinetic parameters, discussions about the relative importance of each reaction group and their effects on chain branching in the oxidation reaction pathways of hydrocarbons are presented. These results are then compared to similar processes in alkyl and alkylperoxy radicals. Where discrepancies are found among these three radical systems, discussions about possible causes are presented. Of particular interest is the observation that 1,6 H-migration reactions are not the dominant pathway in alkoxy radicals, as they are in both alkyl and alkylperoxy radicals, at low temperatures. However, these H-migrations are expected to play a larger role in reaction mechanisms than previously believed, particularly at atmospherically relevant temperatures. This will lead to greater diversity in the intermediate and end product species, which will in turn add complexity to other atmospheric processes, such as aerosol formation and tropospheric ozone production. The current work significantly extends the range of alkoxy radicals that are relevant to models for new fuel systems. Based on the results of this study, recommendations regarding the selection of model systems for future studies are presented.

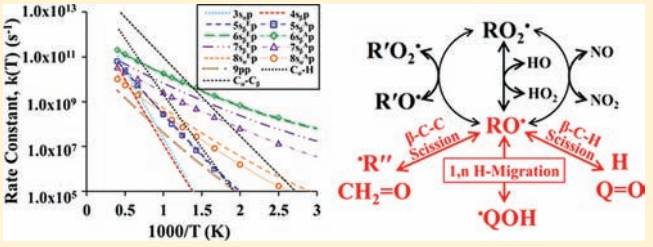

1. INTRODUCTION

Atmospheric decomposition of volatile organic compounds (VOC) has long been known to be responsible for the formation of tropospheric ozone in the presence of NO_x.[1] The general mechanism for how these species break down under atmospheric conditions has been extensively studied (Figure 1). More recently, interest in certain VOCs as possible alternative fuels has begun to shift the focus toward determining their reaction pathways in combustion systems.[2] In both systems, alkyl radicals are formed either by the abstraction of a hydrogen by hydroxyl radicals or by bond scission reactions. These radicals then react with O_2 to form alkylperoxy radicals (reaction 1, Figure 1), which can then undergo unimolecular isomerization reactions to form hydroperoxyalkyl radicals (reaction 3, Figure 1) or concerted elimination reactions to form olefins and HO_2 (reaction 2, Figure 1), or can react with other alkylperoxy radicals, $^{\bullet}OH$, or NO to form an alkoxy radical (reactions 8−10, respectively, Figure 1).[3] In the presence of sufficient NO, reaction 10 is the dominant pathway. Subsequent reactions involving alkoxy radicals lead to significant chain branching and are responsible for the composition and relative concentrations of the first generation of end products. Alkoxy radicals are believed to participate in one of three primary reactions. The first is the reaction with O_2, forming a carbonyl (Q═O) and HO_2 (reaction 11, Figure 1).[4] The second is a unimolecular decomposition reaction involving scission of the α-C−C bond, yielding a shorter alkyl radical (R″) and an aldehyde (CH_2═O) (reaction 13, Figure 1).[5] The final reaction type is a unimolecular isomerization in which a hydrogen atom migrates from the alkyl chain to the oxygen atom (reaction 14, Figure 1); these reactions are referred to as hydrogen-migration reactions.[6] The relative importance of each of these pathways varies, depending on the pressure and temperature conditions in which the reaction takes place. Several reviews have been written on the importance of alkoxy radicals in the oxidation mechanism of hydrocarbons, particularly under atmospheric conditions.[3,7,8] However, little attention has been given to their role in combustion reaction pathways.

Due to the reactive nature of the radical intermediate species, experimental studies utilize product analysis, resulting in rate coefficients that are expressed relative to the reaction between the alkoxy radical and O_2. Although there is a large body of work on decomposition reactions, the experimental literature on H-migrations in alkoxy radicals is limited to reactions involving

Received: May 25, 2011
Published: September 29, 2011

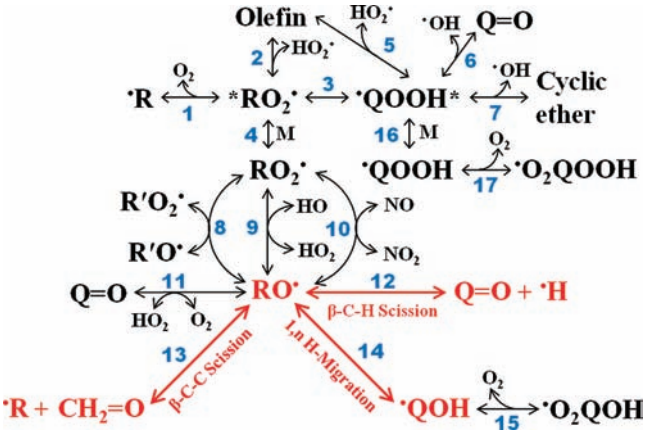

Figure 1. Some of the important reactions (reactions 1−17) that are present in the hydrocarbon oxidization mechanism. The series of reactions shown in red is the focus of this study.

butoxyl, 1- and 2-pentoxyl, and 5-methyl-2-hexoxyl.[8−15] These particular radicals have been selected because they are the smallest molecules that are capable of undergoing 1,5 H-migration reactions involving the transfer of primary, secondary, and tertiary hydrogen atoms.

The discussion of H-migration reactions often relies on a conceptual framework developed by Benson in his work on the alkyl radicals.[16] According to this model, the activation energy, E_a, for H-migration reactions can be estimated on the basis of structural similarities to other reactions and compounds:

$$E_a = E_{strain} + E_{abs}$$

Due to the cyclic nature of H-migration transition-state species, the energy required to form the ring component is approximated by the ring strain of an $(n+1)$ cycloalkane, E_{strain}, where n is the total number of carbon and oxygen atoms contained within the ring. The barrier height for the potential energy surface (PES) of the migrating hydrogen is approximated by the activation energy for a bimolecular H-abstraction reaction, E_{abs}, between either an alcohol or alkane and an alkoxy radical (reactions 18 and 19).

$$R_1OH + R_2O^\bullet \leftrightarrow {}^\bullet Q_1OH + R_2OH \quad (18)$$

or

$$R_1 + R_2O^\bullet \leftrightarrow {}^\bullet Q_1 + R_2OH \quad (19)$$

Based on this model, the 1,5 H-migration reactions, which should exhibit ring strain energies similar to cyclohexane, are expected to have the lowest barrier heights. Later work by Mereau et al.,[5,17] Somnitz et al.,[18] Johnson et al.,[9] Atkinson et al.,[3] as well as Vereecken and Peeters[6,19−21] expanded on this concept to develop a structure−activity relationship (SAR) method for estimating unknown kinetic parameters on the basis of the moieties present on the radical and the site of the migrating hydrogen. Similar SAR studies have also been conducted for H-migrations in alkyl and alkylperoxy radicals.[22−24] Because the 1,5 H-migration is expected to have the lowest barrier, most of the above alkoxy radical SAR studies do not include a ring strain component and instead only predict the 1,5 H-migration reaction. However, the recent study by Vereecken and Peeters does include consideration of other H-migration types, and as such contains a ring strain component, though it is based on averages of computational work and not cycloalkanes.[6] The ultimate goal of these SAR methods is to reduce the number of input variables needed to predict kinetic parameters, enabling the development of computer models that predict reaction pathways and end product formation for systems that lack experimental values.

However, recent experimental and computational results suggest that the use of the cycloalkane model may result in erroneous predictions of the dominant reaction pathways, for both the alkyl and alkylperoxy systems.[25−28] Tsang et al., while conducting pyrolysis experiments on octyl radicals, found that the 1,6 H-migration reactions have a lower barrier height than the 1,5 H-migrations for large alkyl radicals.[26] Similarly, Baldwin et al. showed that the 1,6 H-migration also has a lower barrier height than the 1,5 H-migration for the alkylperoxy radicals.[25] The findings for both of these mechanistically similar reaction systems raise serious questions about the relative barrier heights of the 1,5 and 1,6 H-migration reactions. However, prior to the recent study by Vereecken and Peeters, both experimental and theoretical studies limited themselves to systems in which either the 1,6 H-migration did not exist (the 1-butoxy or 2-pentoxy radicals) or the 1,6 H-migration involved the abstraction of a primary hydrogen, which has been demonstrated to raise the barrier height by ∼2−3 kcal mol^{-1}.[6,9−15,29] Although Thiriot et al. did mention the possible competitive nature of the 1,6 H-migration, their use of the pentoxy radical means that their results undervalue the relative importance of this pathway for larger alkoxy systems.[29] Vereecken and Peeters also reported on the co-competitive nature of the 1,6 H-migration reaction, this time using the hexoxy radical, and found the barrier height to be slightly higher for the 1,6 than the 1,5 H-migration.[6] Although this result differs from the trends in both the alkyl and alkylperoxy radical H-migration reactions, no explanation for the divergence has yet been reported.

Another problem with the cycloalkane conceptual model is that it treats all secondary abstractable hydrogens as equivalent, meaning that the barrier height for a 1,5 H-migration from a secondary site in a pentoxyoxy radical will be the same as in a hexoxy radical since both involve the movement of a secondary hydrogen. However, our studies on alkyl and alkylperoxy radical H-migration reactions demonstrate a clear and consistent difference in energy between a hydrogen that is on a terminal adjacent carbon and one that is farther down the chain.[27,28] These differences in alkyl and alkylperoxy radicals are large enough to affect the reliability of smaller model systems for the prediction of rate parameters in large hydrocarbon reaction mechanisms. In the case of the small differences in barrier heights reported by Vereecken and Peeters between the 1,5 and 1,6 H-migration barrier heights, the 0.3−0.5 kcal mol^{-1} difference between 1,6 H-migrations involving a terminal adjacent and a nonterminal adjacent hydrogen atom, seen in both the alkyl and alkylperoxy systems, could make the barrier lower for the 1,6 than the 1,5 H-migration.[27,28]

The present study attempts to (1) determine the relative importance of the 1,6 H-migration compared to the 1,5 H-migration in terms of both barrier heights and the overall rate constants; (2) assess possible structural differences between alkyl, alkoxy, and alkylperoxy radicals that may be responsible for any observed differences between the three systems; (3) compare the relative importance of the unimolecular reactions in the hydrocarbon oxidation mechanism that are responsible for the end products and determine how this importance changes with temperature; and (4) address the selection of smaller chain hydrocarbons as models for longer chain molecules and make recommendations for future studies.

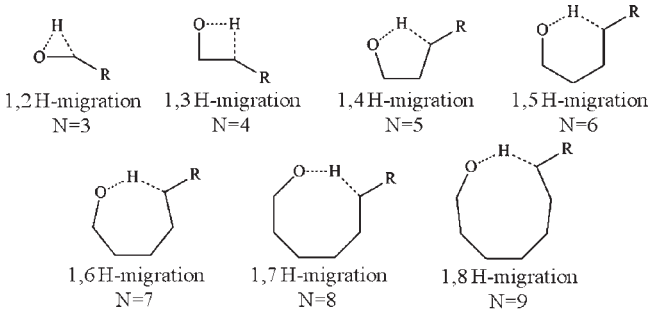

R	H	CH_3	C_nH_{2n+1} n≥2
Symbol	Npp	$Ns_{\alpha}p$	$Ns_{\beta}p$

Figure 2. Diagram of the nomenclature used in this study to describe the H-migration reactions.

2. COMPUTATIONAL METHODOLOGY

Frequency and geometry optimizations for all reactant, product, and transition-state calculations are performed using Gaussian 03 for the CBS-Q and G2 composite methods and the Gaussian 09 suite of programs for the G4 data set.[30,31] The geometries selected for the transition states are based on the corresponding (n+1)-cycloalkane model and the recommendations of previous studies.[27,28] For the cycloheptane- through cyclononane-based systems, the lowest energy conformations reported by Anconi et al., Franco et al., and Wilberg are used.[16,32−34] In each case, the carbon that is selected to serve as a model for the migrating hydrogen is chosen in an attempt to reduce any gauche interactions. The CBS-Q, G2, and G4 composite methods are chosen for their high accuracies, having reported standard deviations of 1.1, 1.0, and 0.8 kcal mol^{-1}, respectively.[35,36] Transition states are confirmed by the presence of a single negative frequency that corresponds to the reaction path of the migrating hydrogen.

Because both the CBS-Q and G2 methods determine low-level HF/6-31G(d) frequencies for zero point energy corrections, additional geometry and frequency calculations are carried out using MP2/6-31G(d) for the reactants, products, and transition-state species. The selection of MP2/6-31G(d) is based on its similarity to the final geometry optimizations of both CBS-Q and G2, which are MP2/6-31G($d^{\ddagger\ddagger}$) and MP2(full)/6-31G(d), respectively.[37] The resulting MP2/6-31G(d) frequencies are used to determine the A-factor and tunneling correction factor, $\kappa(T)$, for the CBS-Q and G2 data sets. For the G4 data set, the B3LYP/GTBas3 frequencies calculated within this composite method are used. Tunneling transmission coefficients are determined using the methods proposed by Wigner and by Skodje and Truhlar (S&T).[38−40] Both methods have the advantage of not requiring full intrinsic reaction coordinate calculations and have been demostrated to give reasonable approximations of the more computationally demanding small-curvature tunneling (SCT) and large-curvature tunneling (LCT) methods.[2,28,41] The exact methods and calculations used for both tunneling methods and the A-factor determination have been described.[27,28] Frequencies and rotational constants are listed in the Supporting Information, Table S1.A,B.

Hydrogen migration reactions are often described using one of two methods: either as an a,b H-migration, where a is the location of the radical on the reactant and b is the location on the product side, or by a method first described by Hardwidge et al., which uses an Ncd format, where N is the number of components in the ring of the transition state, including the hydrogen, and c and d are the types of product and reactant radical sites (p = primary, s = secondary, and t = tertiary) (Figure 2).[42] Following these methods, a 1,6 H-migration in a hexoxy radical would be described as a 7sp transition. This paper will utilize both methods to highlight different aspects of the isomerization reactions. However, the secondary sites using Hardwidge's method will be sublabeled as either s_{α} or s_{β}, depending on the location of the secondary radical site relative to the end of the alkyl chain. The symbol s_{α} will be used for secondary sites that are directly adjacent to the terminal carbon, and s_{β} will represent those that are two or more methylene groups away from a terminus. An A or E superscript will also be used to denote whether the remaining alkyl chain has an axial or equatorial geometry, respectively, when deemed relevant. Thus, the above heptyl 1,6 H-migration reaction with an equatorial transition-state geometry will be indicated as $7s_{\beta}^{E}p$.

3. RESULTS AND DISCUSSION

3.1. Calibration of Computational Methods. The reliability of the CBS-Q, G2, and G4 computational methods used in this study has previously been evaluated by Curtiss et al. and Ochterski et al. using the energies of 125 computationally determined reactions and comparing them to corresponding experimental values.[35−37,43] They reported mean absolute deviations of approximately 1.1, 1.0, and 0.8 kcal mol^{-1} for CBS-Q, G2, and G4, respectively. However, many of these include molecules and reactions types that are different from the unimolecular processes involving alkoxy radicals reported here. As a result, the accuracy relative to alkoxy radicals and alkenes may be higher or lower than these values. In order to determine the reliability of the composite methods for obtaining the thermodynamic properties of alkoxy radicals, five reactions are used to assess the validity of the models used in this study (Table 1), compared to the experimentally determined enthalpy of reaction (ΔH_{rxn}) values.[44] Although the root-mean-squared (rms) deviations of each method, 1.2, 1.7, and 1.3 kcal mol^{-1} for CBS-Q, G2, and G4 respectively, are larger than the above values, the predicted ΔH_{rxn} values are either within or very close to the experimental uncertainty for each reaction (Table 1). This suggests that the values reported here are comparable to experimental results. As for the overall accuracy of the computational methods, the predicted rate coefficients are in reasonable agreement with the available high-temperature values from the literature for the butoxy radical 6pp reaction (Figure 3A).[2,3,14,17,45] However, significant discrepancies occur when the S&T tunneling method is used for temperatures below 400 K, for the G4 data set. The divergence below this temperature is expected on the basis of the findings of Zheng and Trular, as well as our previous study.[28,46] For temperatures below 400 K, which is where the majority of the studies are focused, the Wigner method is recommended over the S&T method, though the resulting transmission coefficient values are expected to be low. On the other hand, both the G2 and G4 methods give results for the C−C bond scission reactions that are in excellent agreement with Somnitz and co-workers but are much higher than the experimental values reported by Baldwin et al. (Figure 3B).[18,45,47,48] Where discrepancies exist, they are likely due to the fact that the experimental rate values are determined relative to the reaction between O_2 and the alkoxy radical. This validates the reliability of both the activation energy and A-factor values and highlights the importance of selecting the right method for determining tunneling at low temperatures.

3.2. Enthalpies of Reaction. All three methods are in reasonable agreement for the reaction enthalpies, particularly for the shorter chain alkoxy radicals. The reaction enthalpies for the CBS-Q method are consistently greater than those obtained with the G2 and G4 composite methods, and this difference appears to increase with the size of the molecule, ranging from 0.4 to 2.5 kcal mol^{-1} for

Table 1. Comparison of Experimental $\Delta H\boxtimes_{rxn}$ with Values Determined Using the Three Computational Methods in This Study (298 K)[44]

		$\Delta H\boxtimes_{rxn}$ (kcal/mol)			
	reaction	exptl[44]	CBS-Q	G2	G4
(1)	$CH_3O^{\bullet} \leftrightarrow {}^{\bullet}CH_2OH$	−9.1 ± 0.5	−8.9	−8.6	−8.4
(2)	$CH_3CH_2O^{\bullet} \leftrightarrow CH_3{}^{\bullet}CHOH$	−9.7 ± 0.8	−10.5	−10.4	−10.0
(3)	$CH_3CH_2O^{\bullet} \leftrightarrow {}^{\bullet}CH_2CH_2OH$	−4.2 ± 1.8	−2.4	−2.6	−2.4
(4)	$CH_3CH_2CH_2O^{\bullet} \leftrightarrow CH_3CH_2{}^{\bullet}CHOH$	−12.2 ± 2.2	−10.3	−9.5	−9.6
(5)	$CH_3{}^{\bullet}CHCH_2OH \leftrightarrow {}^{\bullet}CH_2CH_2CH_2OH$	2.8 ± 2.8	1.7	1.4	1.8
(6)	$CH_3CH_2CH_2O^{\bullet} \leftrightarrow CH_3CH_2{}^{\bullet} + CH_2O$	9.6 ± 2.3	9.6	9.2	10.2
(7)	$CH_3CH_2O^{\bullet} \leftrightarrow CH_3CH_2O$	15.6 ± 0.8	14.2	13.0	15.6
	rms dev		*1.2*	*1.7*	*1.3*

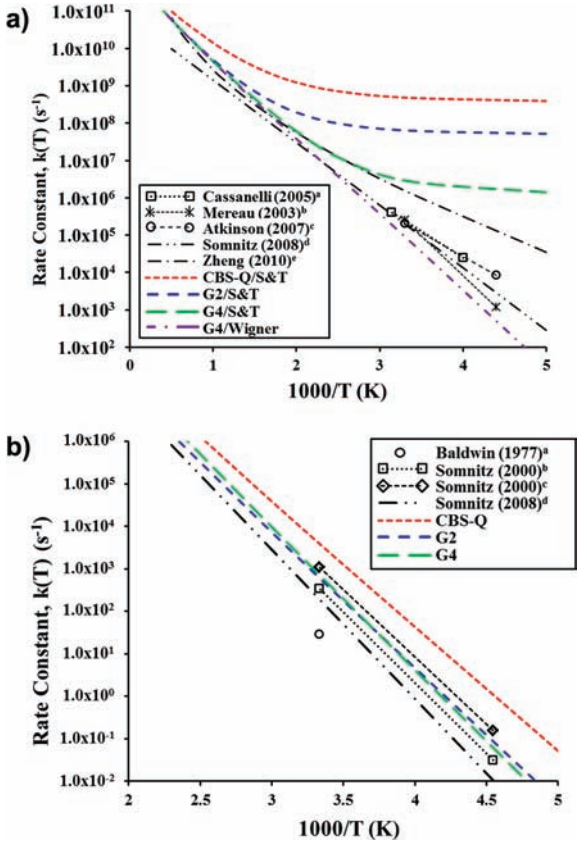

Figure 3. (A) Comparison of the butoxy radical 1,5 H-migration reaction rate coefficients calculated in this study and those reported in other studies ([a]ref 9, [b]ref 14, [c]ref 3, [d]ref 45, [e]ref 2). (B) Comparison of C−C bond scission reaction rate coefficients calculated in this study and those reported in other studies ([a]ref 47, [b]ref 48, [c]ref 18, [d]ref 45). Black lines and symbols represent experimentally derived values.

the propoxy 5pp and heptoxy 6s$_\beta$p reactions, respectively. The G2 and G4 methods demonstrate an excellent agreement, with the G4 generally exhibiting a larger reaction enthalpy than the G2 by roughly 0.5 kcal mol^{-1}.

Within each data set, a clear pattern emerges between the location and the overall stability of the radical site. For each of the

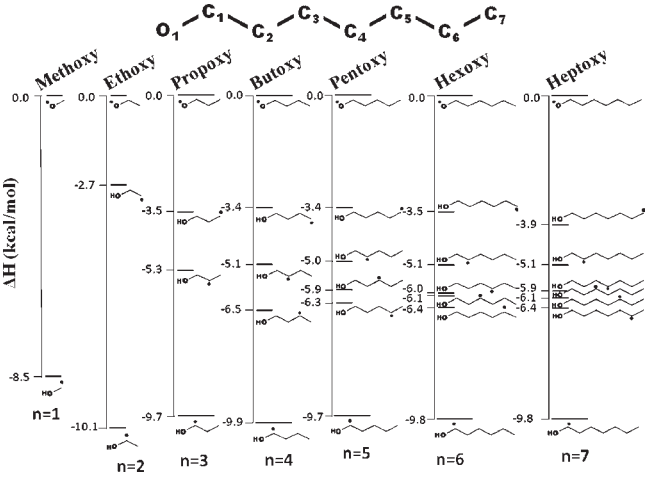

Figure 4. Plot of the G4 enthalpy of reaction for the H-migrations for each alkylperoxy radical (at 0 K), and the labeling scheme used for the discussion of abstraction sites.

alkoxy radicals, the most stable location for the radical is on C_1, which is adjacent to the terminal oxygen group (see Figure 4 and Table 2). As a result, the 1,2 H-migration reactions produce the most stable end product. Of these, the methoxy 3pp reaction has the least exothermic ΔH_{rxn}; further elongation of the alkyl chain leads to an increase by ∼1.5 kcal mol^{-1} to the maximum value for the 3s$_\alpha$p, which then reduces by ∼0.8 and 0.3 kcal mol^{-1} for the G2 and G4 3s$_\beta$p valus, respectively. For the CBS-Q data set, an apparent size-dependent error obscures any difference between *N*sp ΔH_{rxn} values for a given *N*. With ΔH_{rxn} values between −8.5 and −10.5 kcal mol^{-1}, for both the G2 and G4 methods, the alkoxy radical 3sp reactions are significantly more exothermic than the corresponding reactions in alkyl radicals, which have ΔH_{rxn} values ranging from −2.4 to −2.9 kcal mol^{-1}.[28] Moving the product radical site one methylene group down the chain, the result of a 1,3 H-migration, leads to the least exothermic ΔH_{rxn} of all the H-migration reactions. Similar to the 1,2 H-migration reactions, the primary−primary reaction, 4pp, is the least thermodynamically favorable, and the primary to terminal adjacent secondary radical site, 4s$_\alpha$p, is the most favorable of this class of reactions. Further elongation of the carbon chain, the 4s$_\beta$p products, results in a 0.4−0.6 kcal mol^{-1} destabilization. The remaining

Table 2. Activation Energies and Reaction Enthalpies for the Alkoxy Radical H-Migration Reactions (kcal mol^{-1}) at 0 K[a]

	migration type		ΔH_{rxn} (kcal mol^{-1})			$\Delta H^{\ddagger}$ (kcal mol^{-1})				
alkyl radical	1,*n*	*N*ab	CBS-Q	G2	G4	CBS-Q	G2	G4	theor	exptl
methoxy	**1,2**	**3pp**	−9.1 (−8.9)	−8.8 (−8.6)	−8.5 (−8.4)	29.1 (29.1)	29.9 (29.9)	30.1 (30.1)		
ethoxy	**1,2**	**3s$_\alpha$p**	−10.4 (−10.5)	−10.4 (−10.4)	−10.1 (−10.0)	26.9 (26.6)	27.3 (27.0)	27.7 (27.6)		
propoxy	**1,2**	**3s$_\beta$p**	−10.3 (−10.3)	−9.6 (−9.5)	−9.7 (−9.6)	27.0 (26.8)	28.0 (27.8)	28.0 (27.9)		
butoxy	**1,2**	**3s$_\beta$p**	−10.6 (−10.6)	−9.6 (−9.5)	−9.9 (−9.7)	26.8 (26.6)	28.0 (27.8)	27.8 (27.8)	25.2[50]	
pentoxy	**1,2**	**3s$_\beta$p**	−10.4 (−10.4)	−9.6 (−9.5)	−9.7 (−9.6)	26.9 (26.7)	28.0 (27.8)	27.9 (27.9)		
hexoxy	**1,2**	**3s$_\beta$p**	−11.1 (−11.1)	−9.6 (−9.5)	−9.8 (−9.7)	25.9 (25.7)	28.0 (27.8)	27.8 (27.8)		
heptoxy	**1,2**	**3s$_\beta$p**	−11.1 (−11.1)	−9.6 (−9.5)	−9.8 (−9.7)	26.0 (25.7)	27.9 (27.8)	27.8 (27.8)		
ethoxy	**1,3**	**4pp**	−2.5 (−2.4)	−2.8 (−2.6)	−2.7 (−2.4)	27.8 (27.2)	28.8 (28.3)	29.4 (28.9)		
propoxy	**1,3**	**4s$_\alpha$p**	−5.6 (−5.3)	−4.9 (−4.5)	−5.3 (−4.9)	25.1 (24.7)	27.0 (26.6)	27.1 (26.7)		
butoxy	**1,3**	**4s$_\beta$p**	−5.3 (−5.1)	−4.5 (−4.2)	−5.1 (−4.7)	24.9 (24.5)	26.7 (26.3)	26.7 (26.3)	24.8[50]	
pentoxy	**1,3**	**4s$_\beta$p**	−5.6 (−5.4)	−4.5 (−4.2)	−5.0 (−4.6)	24.9 (24.4)	26.7 (26.2)	26.8 (26.4)		
hexoxy	**1,3**	**4s$_\beta$p**	−6.6 (−6.4)	−4.5 (−4.2)	−5.1 (−4.7)	23.6 (23.1)	26.7 (26.2)	26.7 (26.3)		
heptoxy	**1,3**	**4s$_\beta$p**	−6.3 (−6.1)	−4.5 (−4.3)	−5.1 (−4.7)	23.8 (23.3)	26.6 (26.2)	26.6 (26.3)		
propoxy	**1,4**	**5pp**	−3.9 (−3.6)	−3.4 (−3.1)	−3.5 (−3.1)	19.5 (18.7)	21.3 (20.6)	21.4 (20.7)	20.2[6]	
butoxy^E	**1,4**	**5s$_\alpha^E$p**	−6.6 (−6.3)	−5.9 (−5.6)	−6.5 (−6.1)	16.3 (15.7)	18.3 (17.6)	18.1 (17.6)	15.3,[50] 16.7,[6] 19.8[2]	
pentoxy^E	**1,4**	**5s$_\beta^E$p**	−6.0 (−5.8)	−5.5 (−5.3)	−5.9 (−5.6)	16.4 (15.8)	18.1 (17.5)	18.1 (17.5)		
hexoxy^E	**1,4**	**5s$_\beta^E$p**	−7.6 (−7.4)	−5.5 (−5.3)	−6.1 (−5.7)	14.4 (13.7)	18.0 (17.4)	18.0 (17.4)		
heptoxy^E	**1,4**	**5s$_\beta^E$p**	−7.7 (−7.6)	−5.5 (−5.3)	−6.1 (−5.7)	14.0 (13.3)	18.0 (17.4)	17.9 (17.4)		
butoxy^A	**1,4**	**5s$_\alpha^A$p**	−6.6 (−6.3)	−5.9 (−5.6)	−6.5 (−6.1)	16.6 (15.9)	18.6 (17.9)	18.6 (18.0)		
pentoxy^A	**1,4**	**5s$_\beta^A$p**	−6.0 (−5.8)	−5.5 (−5.3)	−5.9 (−5.6)	16.7 (16.0)	18.3 (17.6)	18.4 (17.8)		
hexoxy^A	**1,4**	**5s$_\beta^A$p**	−7.6 (−7.4)	−5.5 (−5.3)	−6.1 (−5.7)	14.3 (13.6)	18.2 (17.5)	18.3 (17.7)		
heptoxy^A	**1,4**	**5s$_\beta^A$p**	−7.7 (−7.6)	−5.5 (−5.3)	−6.1 (−5.7)	13.2 (12.5)	18.1 (17.5)	18.2 (17.6)		
butoxy	**1,5**	**6pp**	−3.7 (−3.5)	−3.0 (−2.8)	−3.4 (−3.0)	8.7 (7.7)	10.8 (9.9)	10.4 (9.5)	8.6,[6] 9.2,[50] 9.9,[17] 11.3,[45] 11.9,[2] 13.2[45,48]	7.3[9]
pentoxy^E	**1,5**	**6s$_\alpha^E$p**	−6.7 (−6.5)	−5.7 (−5.4)	−6.3 (−5.9)	6.3 (5.5)	8.5 (7.6)	8.3 (7.5)	6.2,[6] 7.5,[17] 7.8,[17] 8.1[18]	5.8[9]
hexoxy^E	**1,5**	**6s$_\beta^E$p**	−7.2 (−7.1)	−5.4 (−5.1)	−6.0 (−5.6)	4.4 (3.6)	8.2 (7.3)	7.9 (7.1)	7.6[17]	
heptoxy^E	**1,5**	**6s$_\beta^E$p**	−8.1 (−7.9)	−5.4 (−5.1)	−5.9 (−5.6)	2.5 (1.6)	8.0 (7.2)	7.8 (7.1)		
pentoxy^A	**1,5**	**6s$_\alpha^A$p**	−6.7 (−6.5)	−5.7 (−5.4)	−6.3 (−5.9)	6.7 (5.8)	8.6 (7.8)	8.5 (7.7)		
hexoxy^A	**1,5**	**6s$_\beta^A$p**	−7.2 (−7.1)	−5.4 (−5.1)	−6.0 (−5.6)	4.9 (4.0)	8.1 (7.3)	7.9 (7.1)		
heptoxy^A	**1,5**	**6s$_\beta^A$p**	−8.1 (−7.9)	−5.4 (−5.1)	−5.9 (−5.6)	2.3 (1.4)	8.0 (7.1)	7.8 (7.0)		
pentoxy	**1,6**	**7pp**	−3.7 (−3.5)	−3.2 (−2.9)	−3.4 (−3.0)	9.6 (8.5)	10.9 (9.8)	10.8 (9.7)	8.9[6]	
hexoxy^E	**1,6**	**7s$_\alpha^E$p**	−7.8 (−7.5)	−5.8 (−5.5)	−6.4 (−6.0)	5.4 (4.5)	8.2 (7.2)	8.1 (7.3)	6.3[6]	
heptoxy^E	**1,6**	**7s$_\beta^E$p**	−7.3 (−7.2)	−5.5 (−5.2)	−6.1 (−5.7)	3.8 (2.8)	7.8 (6.9)	7.8 (6.9)		
hexoxy^A	**1,6**	**7s$_\alpha^A$p**	−7.8 (−7.5)	−5.8 (−5.5)	−6.4 (−6.0)	5.9 (4.9)	8.8 (7.8)	8.9 (8.0)		
heptoxy^A	**1,6**	**7s$_\beta^A$p**	−7.3 (−7.2)	−5.5 (−5.2)	−6.1 (−5.7)	4.9 (3.8)	8.3 (7.3)	8.6 (7.6)		
hexoxy	**1,7**	**8pp**	−4.3 (−4.1)	−3.2 (−2.9)	−3.5 (−3.1)	12.0 (10.8)	14.0 (12.8)	13.9 (12.8)	11.3[6]	
heptoxy^E	**1,7**	**8s$_\alpha^E$p**	−7.4 (−7.2)	−5.8 (−5.5)	−6.4 (−6.0)	8.3 (7.2)	11.2 (10.2)	11.2 (10.2)	8.6[6]	
heptoxy^A	**1,7**	**8s$_\alpha^A$p**	−7.4 (−7.2)	−5.8 (−5.5)	−6.4 (−6.0)	8.8 (7.7)	11.8 (10.7)	11.9 (10.8)		
heptoxy	**1,8**	**9pp**	−4.6 (−4.5)	−3.4 (−3.2)	−3.9 (−3.5)	12.6 (11.2)	14.8 (13.6)	14.8 (13.6)	13.0[6]	

[a] Values in parentheses are at 298 K. Energies are relative to the reactant alkoxy radical for each molecule.

H-migration reaction products all follow a similar pattern, with the *N*pp product being the least exothermic and the *N*s$_\alpha$p being ∼2.5−3 kcal mol^{-1} more stable; further elongation of the alkyl chain, the *N*s$_\beta$p, causes a ∼0.3 kcal mol^{-1} destabilization. The 1,5 through 1,8 H-migrations all exhibit similar ΔH_{rxn} values for a given abstraction site type (i.e., p, s$_\alpha$, or s$_\beta$p). These results suggest that both a terminal oxygen and a terminal carbon group affect the stability of not only the adjacent site but also the β-methylene group.

A similar pattern in reaction enthalpies is observed for the unimolecular bond scission reactions. For the C−H bond scission reactions, in particular, the effect that each sequential elongation of the chain has on the ΔH_{rxn} is quite dramatic. For the C−H bond scission in the methoxy radical, the lack of additional alkyl groups on C$_1$ results in the most endothermic reactions of the entire data set reported here. The addition of a single methyl group reduces the ΔH_{rxn} by ∼5 kcal mol^{-1} for each composite method. In each case, the C−H bond scission reaction enthalpy for propoxy is larger than that for ethoxy by between 0.5 and 1.1 kcal mol^{-1}, depending on the method used. However, further elongation leads to a net decrease for the CBS-Q, a continuous increase for G4, and a constant value for the G2 data set (Table 3). For the C−C bond scission reactions, a

Table 3. Activation Energies and Reaction Enthalpies for the Alkoxy Radical Bond Scission Reactions (kcal mol^{-1}) at 0 K[a]

	ΔH_{rxn} (kcal mol^{-1})			$\Delta H^{\ddagger}$ (kcal mol^{-1})				
bond scission reaction	CBS-Q	G2	G4	CBS-Q	G2	G4	theor	exptl
RO• ↔ Q=O + H•								
$CH_3O• \leftrightarrow CH_2O + H•$	18.6 (19.4)	18.0 (18.8)	19.8 (20.6)	22.1 (22.3)	22.8 (23.0)	22.8 (23.1)		
$CH_3CH_2O• \leftrightarrow CH_3CHO + H•$	13.7 (14.2)	12.4 (13.0)	14.9 (15.6)	19.2 (19.0)	19.4 (19.4)	19.9 (20.0)	16.7,[54] 20.0,[52] 20.1[55]	
$CH_3CH_2CH_2O• \leftrightarrow CH_3CH_2CHO + H•$	14.2 (14.8)	13.5 (14.2)	16.0 (16.6)	19.1 (19.0)	20.0 (20.0)	20.1 (20.3)		
$CH_3(CH_2)_2CH_2O• \leftrightarrow CH_3(CH_2)_2CHO + H•$	14.1 (14.7)	13.5 (14.1)	16.1 (16.8)	19.0 (19.0)	20.1 (20.0)	20.1 (20.3)	22.7[50]	
$CH_3(CH_2)_3CH_2O• \leftrightarrow CH_3(CH_2)_3CHO + H•$	14.2 (14.7)	13.5 (14.0)	16.5 (17.1)	19.0 (18.9)	20.0 (20.0)	20.2 (20.3)		
$CH_3(CH_2)_4CH_2O• \leftrightarrow CH_3(CH_2)_4CHO + H•$	13.2 (13.8)	13.5 (14.0)	16.7 (17.4)	18.0 (17.9)	20.0 (20.0)	20.1 (20.2)		
$CH_3(CH_2)_5CH_2O• \leftrightarrow CH_3(CH_2)_5CHO + H•$	13.1 (13.7)	13.5 (14.0)	17.0 (17.7)	18.2 (18.1)	20.0 (20.0)	20.0 (20.2)		
RO• ↔ •R′ + CH_2O								
$CH_3CH_2O• \leftrightarrow •CH_3 + CH_2O$	9.1 (10.2)	7.9 (9.0)	9.9 (11.0)	15.6 (15.6)	16.1 (16.1)	16.6 (16.9)	14.0,[54] 16.1,[21] 17.3,[18] 18.3,[52] 18.7,[48] 18.8[21]	18.2,[8] 21.6[47]
$CH_3CH_2CH_2O• \leftrightarrow CH_3CH_2•CH_2O$	8.8 (9.6)	8.4 (9.2)	9.4 (10.2)	13.0 (13.1)	14.1 (14.2)	14.3 (14.6)	14.5,[18] 14.9,[21] 15.1[48]	15.7,[8] 19.5[47]
$CH_3(CH_2)_2CH_2O• \leftrightarrow CH_3CH_2CH_2• + CH_2O$	9.9 (10.4)	9.1 (9.6)	9.8 (10.6)	13.4 (13.5)	14.5 (14.6)	14.7 (15.0)	14.2,[48] 14.5,[45] 15.0,[18,21] 16.0,[50] 16.7,[45] 16.8[48]	15.8,[8] 19.1[47]
$CH_3(CH_2)_3CH_2O• \leftrightarrow CH_3(CH_2)_2• + CH_2O$	10.5 (11.0)	9.1 (9.6)	10.1 (10.7)	13.2 (13.3)	14.3 (14.5)	14.7 (14.9)	14.8,[21] 14.9[18]	15.1[8]
$CH_3(CH_2)_4CH_2O• \leftrightarrow CH_3(CH_2)_3• + CH_2O$	9.4 (9.9)	9.2 (9.7)	10.0 (10.7)	12.2 (12.3)	14.3 (14.4)	14.6 (14.8)		
$CH_3(CH_2)_5CH_2O• \leftrightarrow CH_3(CH_2)_4• + CH_2O$	9.0 (9.1)	9.2 (9.7)	10.1 (10.7)	12.5 (12.5)	14.3 (14.4)	14.5 (14.8)		

[a] Values in parentheses are at 298 K. Energies are relative to the primary alkyl radical for each molecule.

dx.doi.org/10.1021/ja204806b J. Am. Chem. Soc. 2011, 133, 18208–18219

slightly different trend than either the H-migrations or C−H bond scission reactions is observed. For these reactions, the presence of an additional methyl group at the bond scission site again produces the most stable product, but unlike the previous two reaction groups, further elongation of the chain yields ΔH_{rxn} values that are roughly equivalent to those for the ethoxy radical.

Overall, the reaction enthalpies for the H-migration reactions are more exothermic than those for the bond scission reactions. As a result, the H-migration reactions are more thermodynamically favorable, and, if equilibrium is established, the reactions will favor the transfer of a hydrogen atom along the alkyl chain to the terminal oxygen. However, for the bond scission reactions, because the reaction results in the formation of two new molecules, the forward direction of these reactions is also expected to be favored. For both sets of unimolecular reactions, the reactions that result in the formation of a terminal carbon radical have the least favorable ΔH_{rxn} values. Also, for each group reactions, there is a clear difference in reaction enthalpies between those reactions that involve a terminal adjacent secondary site and those that involve a nonterminal adjacent secondary site. These trends are consistent with our previous findings on alkyl and alkylperoxy radicals, which also exhibited a significant difference between the primary and secondary sites and, to a lesser extent, between the α- and β-secondary radical sites.[27,28] This means that the oversimplification of treating all secondary sites as having equivalent reaction enthalpies for a given reaction type could lead to significant errors in the predicted behavior and relative end product formation of these reactions.

3.3. Activation Energies. On the basis of the cycloalkane conceptual model that is commonly used to predict the relative importance of the H-migration reactions, the activation energies are expected to mirror the ring strain energies of (n+1)-cycloalkanes (Figure 2). This means that the activation energies are expected to decrease with each successive increase in transition-state ring size between the 1,2 and 1,5 H-migrations, after which the barrier height will increase with each further expansion of the ring. As a result, the 1,5 H-migration reaction transition states will have ring strain components roughly equal to that of cyclohexane, and the 1,6 H-migration reaction transition states will have ring strain components equivalent to that of cycloheptane. The difference between the activation energies of the 1,5 and 1,6 H-migration reactions is therefore predicted to be approximately 6 kcal mol^{-1}.[16,24] However, for both the alkyl and alkylperoxy radicals, the activation energies for the H-migration reactions do not follow this trend. In the case of alkylperoxy radicals, early work by Baldwin and co-workers demonstrated that the 1,6 H-migration reaction has a 4.8 kcal mol^{-1} lower barrier height than the 1,5 H-migration.[25] Similarly, recent shock tube experiments by Tsang and co-workers suggested the 1,6 H-migrations in octyl radicals are approximately equal in energy to the 1,5 reactions.[26] Our own computational studies confirm the results Baldwin et al., with the 1,6 H-migration being between 1.0 and 1.2 kcal mol^{-1} lower in energy than the 1,5 H-migration in alkylperoxy radicals, using the G2 composite method. However, for the alkyl radicals, the 1,6 H-migration was found to be between 0.4 and 0.7 kcal mol^{-1} lower in energy than the 1,5 H-migration, using either the G2 or G4 methods.[27,28] These lower than expected barrier heights alter the perceived importance of each of the different reaction pathways. As a result, the 1,5 and 1,6 H-migrations will be co-competitive at high temperatures; at low temperatures, the lower activation energies for the 1,6 H-migrations lead to an alteration in the dominant

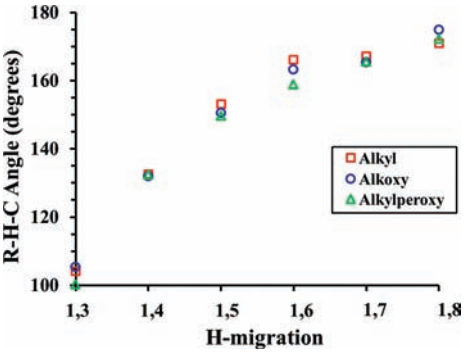

Figure 5. Graph of the MP2/6-31G(d) angles between the migrating hydrogen and the bridge head sites for the alkyl, alkoxy, and alkylperoxy H-migration reactions. Values for the alkyl and alkylperoxy are taken from our other recent studies.[27,28]

pathway for both systems. A possible cause for this divergence from the predicted values is the result of inaccuracies in one of the underlying assumptions to the (n+1)-cycloalkane conceptual model. It can be argued that, for the smaller transition-state rings, the ability of cycloalkanes to predict the ring strain associated with the formation of the transition state is accurate. Unfortunately, these estimation methods also rely on bimolecular H-abstraction reactions, involving similar radicals and abstraction sites, to model the PES of the migrating hydrogen. For alkoxy radical H-migrations, the bimolecular reaction between an alkoxy radical and an alkane, leading to the formation of an alcohol and an alkyl radical, is used as the model system (reaction 19). In the bimolecular reactions, the hydrogen atoms move along a nearly linear path from one site to the other; however, the ring structure of the H-migration transition state alters the PES, causing the migrating hydrogen to move along a different, higher energy pathway. As transition-state size increases, the ring strain associated with its formation decreases, enabling the migrating hydrogen to traverse a PES that is more accurately modeled by the bimolecular H-abstraction reactions, primarily due to the broadening of the O−H−C bond angle in the transition state (Figures 2 and 5). For both the alkyl and alkylperoxy radical H-migration reactions, the interplay between these energetic components results in a failure within the model to predict the most favorable pathway for large hydrocarbon radicals at low temperatures, where the 1,6 H-migration reaction has a higher rate constant than the 1,5. However, this is not the case for the alkoxy radicals. For the computational methods used here, the 1,6 H-migration reactions have either an equivalent barrier, as is the case for both the G4 and G2 data sets, or a barrier that is approximately 1.0 kcal mol^{-1} higher than that of the 1,5 H-migration reactions, as seen in the CBS-Q data (Figure 6, and Table 2). In each case, the cycloalkane model fails to accurately predict the relative difference in barrier height between the 1,5 and 1,6 H-migration reactions. When combined with the A-factor, as will be discussed in the next section, the ability of the cycloalkane model to predict the relative importance of the rate constants fails for both the alkylperoxy and alkyl radicals, but for the alkoxy radicals, the 1,5 H-migration remains the dominant pathway, though not by as much as predicted.

These discrepancies between the mechanistically similar H-migrations in alkyl, alkoxy, and alkylperoxy radicals raise the question of what differences between the three radical groups could lead to the observed variations in the reaction pathways.

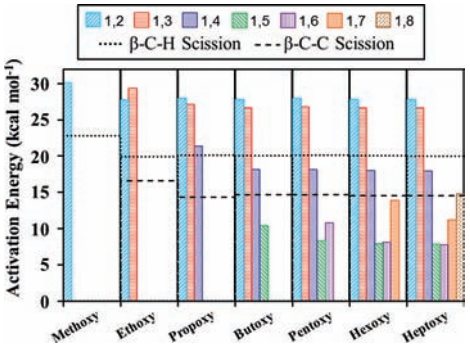

Figure 6. Bar graph of the activation energies for the bond scission reactions and the *N*pp and *N*s^{E}p H-migrations reactions for each of the alkoxy radicals.

One possible explanation can be found by comparing the angles by which the hydrogen atoms migrate in each H-migration and the angles by which a hydrogen atom moves from one molecule to another in a related bimolecular H-abstraction reaction. Because the bimolecular H-abstraction reactions are not constrained by cyclic structures, the angle between the radical, hydrogen, and abstraction site, the X−H−C angle, should accurately represent the optimal angle for a migrating hydrogen. The larger the differences between the two sets of angles are, the higher the activation energy for the 1,*n* H-migrations should be. Although the X−H−C angles for the H-migration reactions in each of the three radical systems are similar (Figure 5), the same angles for their respective bimolecular analogues are vastly different. In the case of the alkyl radical systems, Dybala-Defratyka et al. reported C−H−C angles of 177.0°, 177.5°, and 179.2° for the ethane/ethyl bimolecular H-abstraction reactions using the MP2/6-31G(d+), MP2(full)/6-31G(d), and B3LYP/6-31G(2df,p) levels of theory, respectively.[49] Both the 1,5 and 1,6 H-migration C−H−C angles differ significantly from the bimolecular angles, with values of approximately 153° and 166°, respectively.[28] Because the angular strain energies decrease at a lower rate, as the ideal value is approached, the pathway the 1,5 H-migration traverses along the model PES will be much higher in energy than for the 1,6. As a result, the 1,6 H-migration has a lower barrier than the 1,5 reaction for alkyl radicals. On the other hand, for the bimolecular reactions involving the alkoxy radicals, Lendvay and Viskolcz reported O−H−C angles of 161.1° and 168.8° for the methoxy/ethanol and methoxy/propane, respectively, using MP2/6-31G(d).[50] This 9−17° reduction in angle, compared to the alkyl radical system, means that the alkoxy 1,5 H-migration O−H−C angle is only 10−17° away from the ideal value, which is significantly less than the 24−26° difference in the alkyl radical 1,5 H-migration C−H−C angles. The smaller deviation in the alkoxy system indicates that the migrating hydrogen will traverse a lower energy pathway along the model PES, resulting in a lower barrier height. This would partially explain why the activation energy for the 1,5 H-migration reaction remains less than or equal to that for the 1,6 H-migration for the alkoxy radicals but not the alkyl or alkylperoxy systems. As a result, the 1,6 H-migration reactions will play a larger role in the overall oxidation and decomposition pathways of long-chain hydrocarbons than has been indicated by previous studies, but not to the same extent as observed in the alkyl or alkylperoxy radicals.

The remaining unimolecular reactions follow trends similar to those predicted by an (*n*+1)-cycloalkane model. The 1,2 and 1,3 H-migration reactions have the highest activation energies and are therefore not expected to contribute meaningfully to the end product formation (Figure 6 and Tables 2 and 3). The values reported here for these reaction groups are in reasonable agreement with those reported by Lendvay and Viskolcz, given the difference in accuracy between their BAC-MP4 and the composite methods used here.[50] Increasing the ring size of the transition state to the 1,4 H-migrations reduces the barrier height by approximately 8−10 kcal mol^{-1} in each of the composite methods. The resulting 17.0−21.4 kcal mol^{-1} activation energies are lower than the 19.4−22.8 kcal mol^{-1} barriers for the C−H bond scission reactions, in the G2 and G4 data sets. The activation energies for the 1,4 H-migrations are in good agreement with the CBS-QB3 values reported by Vereecken and Peeters, but are ∼3 kcal mol^{-1} larger than those reported by Lendvay and Viskolcz.[6,50] At the same time, the C−H bond scission values reported here are 2.6 kcal mol^{-1} lower than those reported by Lendvay and Viskolcz, but are in good agreement with those reported by Zhang et al. and Hoyermann et al.[51,52] As a result, the 1,4 H-migration reactions will not play as significant a role in the overall reaction mechanisms as reported by Lendvay and Viskolcz. Further expansion of the transition-state ring results in the previously discussed 1,5 and 1,6 H-migration reactions. These two reaction groups have the lowest barrier heights and are therefore expected to contribute the most to the end product distribution, particularly at low temperatures. The CBS-Q values for the 1,5 and 1,6 H-migration reactions are in good agreement with the CBS-QB3 values reported by Vereecken and Peeters, but the G2 and G4 values are much higher.[6] The G2 and G4 values for the 1,5 H-migration reactions are also significantly higher than the values experimentally derived by Johnson et al.; however, the resulting rate constant of their study and those reported here (see discussion below) are in excellent agreement.[9] This, when combined with the good agreement with other literature values, suggests that the values reported here are accurate.[2,17,18,45,50] The C−C bond scission reactions are also expected to make a significant contribution to the end product formation. Although their barrier heights are roughly 6.0 kcal mol^{-1} higher than those of either the 1,5 or 1,6 H-migrations, their transition states require far less rearrangement and will therefore have a higher *A*-factor. The activation energies reported here for the C−C bond scission are in good agreement with the recent CBS-QB3 data of Vereecken and Peeters.[21] The majority of the other theoretical values are within rms error of the composite methods in this study (Tables 1 and 3).[18,45,48,50] It is interesting to note that the 1,4 H-migration activation energies reported by Lendvay and Viskolcz are lower than those reported here, and at the same time, the C−C bond scissions are higher.[50] These differences have a significant impact on the relative importance of each of these two pathways. Finally, the 1,7 and 1,8 H-migration transition states both have higher activation energies than those for the 1,5 and 1,6 reactions. As a result, their contributions to the end product composition are expected to be minimal.

On the basis of the relative barrier height of each of the unimolecular reactions, the 1,5 H-migrations are expected to be the dominant pathways, with the 1,6 H-migrations contributing significantly to the overall mechanism. The C−C bond scission reactions, which have less restricted transition states, will also contribute to the end products. Because the 1,4 H-migrations have both a higher activation energy than the C−C bond scission reactions and a lower *A*-factor, they will not be a competitive reaction pathway at any temperature. This final point is in direct

conflict with the predictions of Lendvay and Viskolcz, who stated that the 1,4 H-migration reactions would compete with the C−C scission reactions.[50] The remaining unimolecular reactions will not contribute significantly to the overall combustion and atmospheric decomposition mechanisms of hydrocarbons.

3.4. Rates. Although activation energies are a good indicator of the relative importance of each reaction pathway, other factors, such as tunneling and the change in entropy required to form the transition states, can also have a significant impact on the rate constant. As Figures 7 and 8 suggest, there is a complex interplay between the various possible pathways that changes with temperature. At high temperatures, tunneling becomes negligible and the differences between barrier heights play a less significant role in determining the dominant reaction pathways. Instead, the amount of rearrangement required to form the transition state, indicated by the *A*-factor (Table S3.A,B), has the largest effect on rate constants. As a result, the unimolecular C−C bond scission reactions are the dominant reaction pathways at high temperatures, regardless of the method used to determine tunneling. A comparison of Figures 7C and 8C shows that, at 1000 K, the C−C bond scission reaction will account for the majority of the decomposition mechanism of alkoxy radicals. The 6pp and 6sp reactions will also act as competitive pathways, though the former, avaliable only to the butoxy radicals, will do so to a much lesser extent. It is also interesting to note that, even at this relatively high temperature, the 1,6 H-migration will make a measurable contribution to the overall mechanism for the hexoxy and larger alkoxy radicals. As expected, the *N*pp rate coefficients are significantly lower than those of the *N*sp, which implies that the selection of the commonly used butoxy or even the less common pentoxy radical systems will not yield reliable information concerning the relative importance of the various alkoxy radical reactions for the combustion and decomposition pathways of larger hydrocarbons. As the temperature decreases, both tunneling and barrier heights become increasingly important in determining the dominant reaction pathways.

There is a switch in the dominant reaction pathway from the C−C bond scission to the 1,5 H-migration at a temperature, whose predicted value depends on the method used to determine the tunneling. Using the S&T tunneling constants with the G4 data, the change occurs between 700 and 800 K for the heptoxy radical, whereas using the Wigner method the switch happens between 600 and 700 K. The former method has been demonstrated to give results that are in better agreement with the more accurate SCT and LCT methods down to ∼400 K, after which it tends to overpredict the tunneling transmission coefficient.[28,41,46] The Wigner method, which is dependent only on the imaginary frequency of the transition state and not the actual shape or height of the barrier, will underpredict the role of tunneling at all temperatures, but it is more reliable than the S&T method for temperatures below 400 K. As the temperature decreases, the relative importance of the C−C bond scission reactions quickly diminishes, and the 1,5 H-migration become the dominant unimolecular reaction pathway. Although it is never the dominant pathway, the $7s^{E}p$ H-migration reaction has rate coefficients that are roughly 30% of those of the 6sp, making it a competitive pathway that makes a significant contribution to the end product composition.

It is interesting to note that, although the butoxy radical has been the predominant system used in previous theoretical studies, the predicted importance of the 6pp reaction relative to the C−C bond scission is significantly different from those of alkoxy

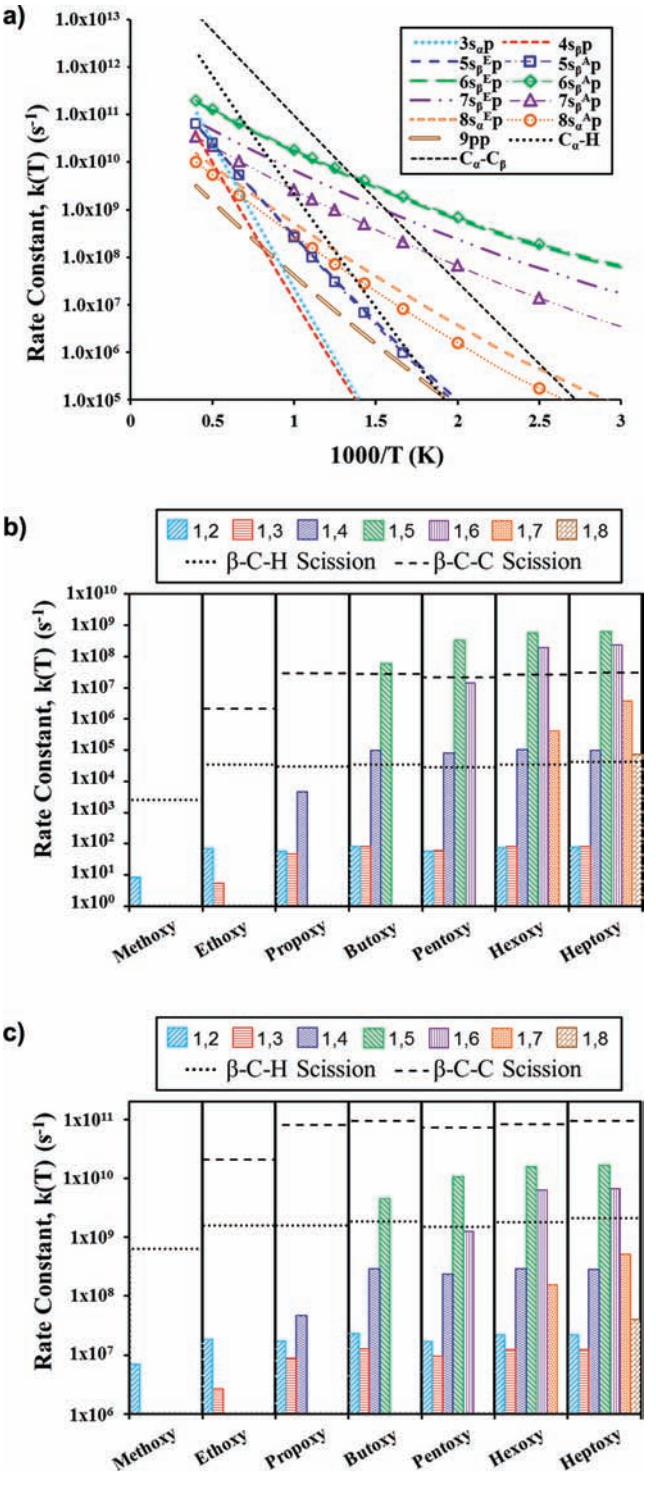

Figure 7. (A) Plot of the G4 rate constants, $k(T)$, for the heptoxy radical, using the Skodje−Truhlar method for predicting the effect of tunneling. (B) G4 rate constants at 500 K using the S&T tunneling method. (C) G4 rate constants at 1000 K using the S&T tunneling method.

radicals that undergo a 6sp H-migration, particularly if the more conservative Wigner tunneling approximation is used (Figure 8B). Additionally, the use of the pentoxy radical as a model for the reactions in larger alkoxy radical will lead to significant errors in the predicted relative importance of the 1,6 H-migration reactions. As Figures 7B and 8B clearly show, at 500 K, the pentoxy 7pp is

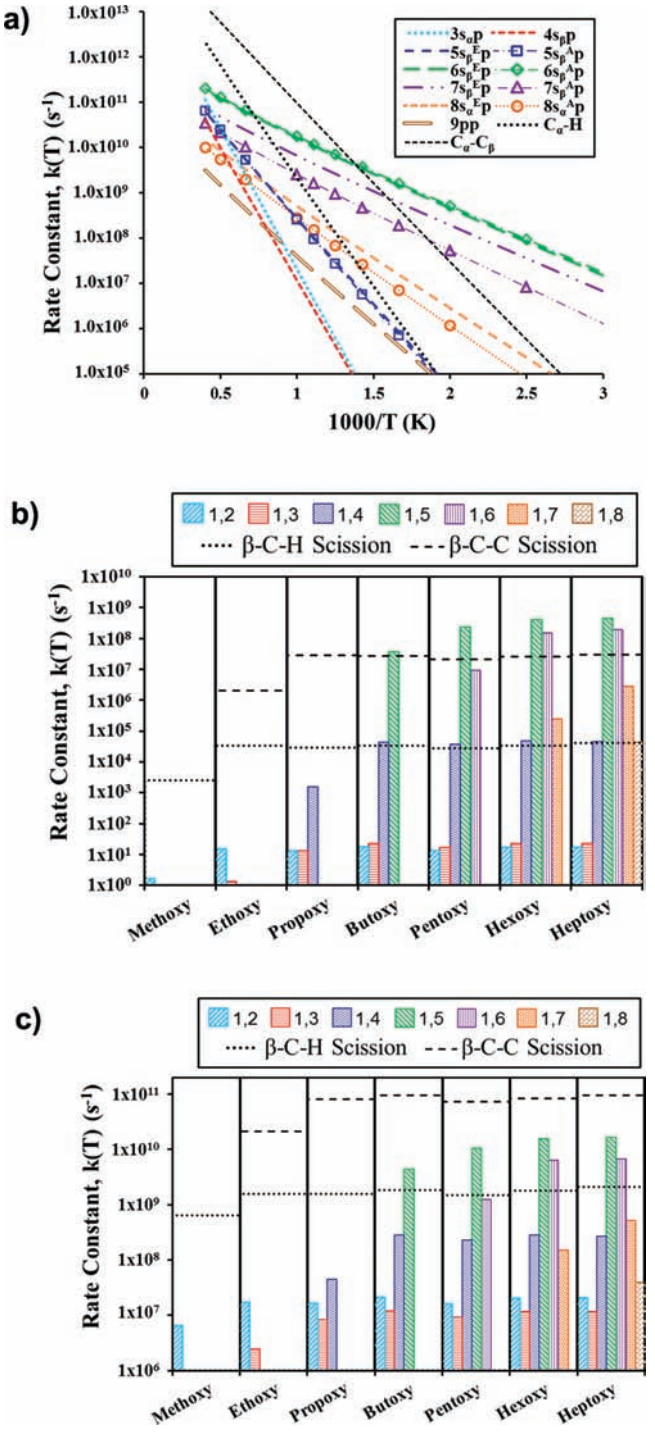

Figure 8. (A) Plot of the G4 rate constants, $k(T)$, for the heptoxy radical, using the Wigner method for predicting the effect of tunneling. (B) G4 rate constants at 500 K using the Wigner tunneling method. (C) G4 rate constants at 1000 K using the Wigner tunneling method.

less important in the determination of end product formation than the C−C bond scission reactions. However, for the hexoxy and heptoxy radicals, the 7sp reaction rate constant is not only roughly an order of magnitude greater than that of the C−C bond scission reaction, but it is also competitive with those of the 1,5 H-migration reactions, and as such will contribute significantly to the end product composition.

Since the dominant reaction pathway involving alkoxy radicals changes with temperature, the atmospheric decomposition and combustion mechanisms of hydrocarbons, under incomplete oxidation conditions, will produce significantly different end products. At high temperatures, once formed, alkoxy radicals will quickly undergo C−C bond scission to form a carbonyl and an alkyl radical. However, at lower temperatures, below ∼700 K, H-migration reactions become dominant, resulting in the formation of hydroxy-substituted alkyl radicals. This will have dramatic ramifications for atmospheric processes involving hydrocarbons. Since both the 1,5 and 1,6 H-migrations are the dominant pathways, the atmospheric oxidation mechanism will branch, yielding two sets of hydroxyalkyl radicals, each with a different radical site. These species can then react with O_2 to form two distinct hydroxyalkylperoxy radicals. Because both the 1,5 and 1,6 H-migration reactions have significantly higher rates than the C−C or C−H bond scission reactions, their role in the atmospheric oxidation mechanism will lead to a greater variety of longer, more oxidized intermediates and end products. These species can in turn affect other atmospheric processes, such as the hydrophilicity of aerosols and tropospheric ozone production.[53]

CONCLUSIONS

The present study investigates all unimolecular reactions involving 1-alkoxy radicals that lead to chain branching in the oxidation mechanism of unbranched hydrocarbons from methoxy through heptoxy. This work reports on (1) the relative importance of the 1,6 H-migration compared to the 1,5 H-migration in determining end product formation; (2) possible structural differences between alkyl, alkoxy, and alkylperoxy radicals that may explain the difference in the relative importance of the 1,5 and 1,6 H-migration reactions; (3) the selection of smaller chain radicals as models for longer chain molecules; and (4) the relative importance of each of the alkoxy unimolecular reactions in the hydrocarbon oxidation mechanism that are responsible for the relative concentrations of end products.

Unlike the alkyl and alkylperoxy radicals, where the 7sp reactions have sufficiently lower activation energies than the 6sp reactions to make them the dominant H-migration reaction at low temperatures, 1,5 H-migration for the alkoxy radical has the lowest barrier of any of the unimolecular reactions. Thus, although the 1,6 reaction will play a significant part in the oxidation mechanism of larger hydrocarbons, the 1,5 is expected to be the dominant H-migration reaction. The observed discrepancy in the trends of the relative barrier heights between the 6sp and 7sp reactions in the alkoxy radicals, as compared to the alkyl and alkylperoxy systems, is a result of differences in the PES of the migrating hydrogen. Although the X−H−C angles by which the migrating hydrogen atom moves from one site to another along the chain are very similar among the three radical systems, the ideal hydrogen-transfer angles, indicated by bimolecular reactions involving an alkane and the corresponding radical, are significantly different. Of the three radical systems, the alkoxy O−H−C angles for the bimolecular H-abstraction are the lowest and hence the closest to the O−H−C angle in the 1,5 H-migration reactions.

The interplay between the various unimolecular reactions is complex and varies with temperature. At high temperatures, the C−C bond scission reactions are the dominant pathway, with the 1,5 H-migration reactions beginning to play a meaningful role in end product composition around 1000 K. Below this temperature,

at roughly 600 and 700 K, the 6pp and 6sp reactions become the dominant pathways for the butoxy and larger alkoxy radicals, respectively. Although they never become the dominant reaction, the $7s^{E}p$ reactions will be competitive with the 6sp at lower temperatures. The remaining unimolecular reactions, other than the C−H bond scission in the methoxy radical, will not make any significant contribution to the end product composition. Of particular interest is the observation that the 1,4 H-migration will not be competitive with the C−C bond scission reactions for any alkoxy radical. This result is in direct conflict with previous computational studies.[50]

Although the 1,6 H-migration is not the dominant pathway, future studies need to include it in their analyses. At low temperatures these reactions may be responsible for as much as 30% of the unimolecular decomposition reactions in larger alkoxy radicals. Also, due to the significant differences between *N*pp and *N*sp reactions, and the lower than expected barrier heights for the 7sp reactions, the use of smaller radicals as analogues for hexoxy and larger alkoxy is not recommended.

■ ASSOCIATED CONTENT

Supporting Information. Complete refs 30, 31, and 53; tabulated frequencies and rotational constants for reactants, products and transition states; tabulated Arrhenius pre-exponential factors for both the forward and reverse reactions; tabulated tunneling transmission coefficients determined using both the Skodje−Truhlar and Wigner methods; tabulated heat capacities; and absolute energies and Cartesian coordinates for the reactants, products, and transition states used in this study. This material is available free of charge via the Internet at http://pubs.acs.org.

■ AUTHOR INFORMATION

Corresponding Author
davisac@purdue.edu;francisc@purdue.edu

■ ACKNOWLEDGMENT

We thank the Purdue Rosen Center for Advanced Computing for their assistance with providing and maintaining the computational resources used for this study.

■ REFERENCES

(1) Finlayson-Pitts, B. J.; Pitts, J. N. *Chemistry of the Upper and Lower Atmosphere*; Academic Press: San Diego, CA, 2000.
(2) Zheng, J. J.; Truhlar, D. G. *Phys. Chem. Chem. Phys.* **2010**, *12*, 7782–7793.
(3) Atkinson, R. *Atmos. Environ.* **2007**, *41*, 8468–8485.
(4) Setokuchi, O.; Sato, M. *J. Phys. Chem. A* **2002**, *106*, 8124–8132.
(5) Mereau, R.; Rayez, M. T.; Caralp, F.; Rayez, J. C. *Phys. Chem. Chem. Phys.* **2000**, *2*, 3765–3772.
(6) Vereecken, L.; Peeters, J. *Phys. Chem. Chem. Phys.* **2010**, *12*, 12608–12620.
(7) Hayes, C. J.; Merle, J. K.; Hadad, C. M. *Advances in Physical Organic Chemistry, Vol. 43*; Academic Press Ltd./Elsevier Science Ltd.: London, 2009; pp 79−134.
(8) Orlando, J. J.; Tyndall, G. S.; Wallington, T. J. *Chem. Rev.* **2003**, *103*, 4657–4689.
(9) Johnson, D.; Cassanelli, P.; Cox, R. A. *J. Phys. Chem. A* **2004**, *108*, 519–523.
(10) Carter, W. P. L.; Lloyd, A. C.; Sprung, J. L.; Pitts, J. N. *Int. J. Chem. Kinet.* **1979**, *11*, 45–101.
(11) Cox, R. A.; Patrick, K. F.; Chant, S. A. *Environ. Sci. Technol.* **1981**, *15*, 587–592.
(12) Niki, H.; Maker, P. D.; Savage, C. M.; Breitenbach, L. P. *J. Phys. Chem.* **1981**, *85*, 2698–2700.
(13) Hein, H.; Hoffmann, A.; Zellner, R. *Phys. Chem. Chem. Phys.* **1999**, *1*, 3743–3752.
(14) Cassanelli, P.; Johnson, D.; Cox, R. A. *Phys. Chem. Chem. Phys.* **2005**, *7*, 3702–3710.
(15) Cassanelli, P.; Cox, R. A.; Orlando, J. J.; Tyndall, G. S. *J. Photochem. Photobiol. A-Chem.* **2006**, *177*, 109–115.
(16) Benson, S. W. *Thermochemical Kinetics*, 2nd ed.; Wiley: New York, 1976.
(17) Mereau, R.; Rayez, M. T.; Caralp, F.; Rayez, J. C. *Phys. Chem. Chem. Phys.* **2003**, *5*, 4828–4833.
(18) Somnitz, H.; Zellner, R. *Phys. Chem. Chem. Phys.* **2000**, *2*, 4319–4325.
(19) Vereecken, L.; Peeters, J. *J. Chem. Phys.* **2003**, *119*, 5159–5170.
(20) Peeters, J.; Fantechi, G.; Vereecken, L. *J. Atmos. Chem.* **2004**, *48*, 59–80.
(21) Vereecken, L.; Peeters, J. *Phys. Chem. Chem. Phys.* **2009**, *11*, 9062–9074.
(22) Matheu, D. M.; Green, W. H., Jr.; Grenda, J. M. *Int. J. Chem. Kinet.* **2003**, *35*, 95–119.
(23) Curran, H. J.; Gaffuri, P.; Pitz, W. J.; Westbrook, C. K. *Combust. Flame* **1998**, *114*, 149–177.
(24) Fish, A. In *Organic Peroxides*; Swern, D., Ed.; Wiley Interscience: New York, 1970; Vol. 1.
(25) Baldwin, R. R.; Hisham, M. W. M.; Walker, R. W. *J. Chem. Soc., Faraday Trans. 1* **1982**, *78*, 1615–1627.
(26) Tsang, W.; McGivern, S.; Manion, J. A. *Proc. Combust. Inst.* **2009**, *32*, 131–138.
(27) Davis, A. C.; Francisco, J. S. *J. Phys. Chem. A* **2010**, *114*, 11492–11505.
(28) Davis, A. C.; Francisco, J. S. *J. Phys. Chem. A* **2011**, *115*, 2966–2977.
(29) Thiriot, E.; Canneaux, S.; Henon, E.; Bohr, F. *React. Kinet. Catal. Lett.* **2005**, *85*, 123–129.
(30) Frisch, M. J.; et al. *Gaussian03*, revision E.01; Gaussian Inc.: Pittsburgh, PA, 2003.
(31) Frisch, M. J.; et al. *Gaussian09*, revision A.1; Gaussian, Inc.: Wallingford, CT, 2009.
(32) Anconi, C. P. A.; Nascimento, C. S., Jr.; Dos Santos, H. F.; De Almeida, W. B. *Chem. Phys. Lett.* **2006**, *418*, 459–466.
(33) Franco, M. L.; Ferreira, D. E.; Dos Santos, H. F.; De Almeida, W. B. *Int. J. Quantum Chem.* **2007**, *107*, 545–555.
(34) Wilberg, K. B. *J. Org. Chem.* **2003**, *68*, 9322–9329.
(35) Ochterski, J. W.; Pererson, G. A.; Wiberg, K. B. *J. Am. Chem. Soc.* **1995**, *117*, 11299–11308.
(36) Curtiss, L. A.; Redfern, P. C.; Raghavachari, K. *J. Chem. Phys.* **2007**, *126*, 084108.
(37) Ochterski, J. W.; Pererson, G. A.; Montgomery, J. A., Jr. *J. Chem. Phys.* **1996**, *104*, 2598–2619.
(38) Wigner *Z. Phys. Chem.* **1932**, *19*, 203.
(39) Skodje, R. T.; Truhlar, D. G.; Garrett, B. C. *J. Phys. Chem.* **1981**, *85*, 3019–3023.
(40) Skodje, R. T.; Truhlar, D. G. *J. Phys. Chem.* **1981**, *85*, 624–628.
(41) Sirjean, B., Wang, H., Tsang, W. Presented at the 6th U.S. National Combustion Meeting Ann Arbor, MI, 2009.
(42) Hardwidge, E. A.; Larson, C. W.; Rabinovitch, B. S. *J. Am. Chem. Soc.* **1970**, *92*, 3278–3283.
(43) Curtiss, L. A.; Raghavachari, K.; Trucks, G. W.; Pople, J. A. *J. Chem. Phys.* **1991**, *94*, 7221–7230.
(44) *CRC Handbook of Chemistry and Physics*; Lide, D. R., Ed.; Taylor and Francis Group LLC: 2009.
(45) Somnitz, H. *Phys. Chem. Chem. Phys.* **2008**, *10*, 965–973.
(46) Zheng, J. J.; Truhlar, D. G. *J. Phys. Chem. A* **2009**, *113*, 11919–11925.
(47) Baldwin, A. C.; Barker, J. R.; Golden, D. M.; Hendry, D. G. *J. Phys. Chem.* **1977**, *81*, 2483–2492.

(48) Somnitz, H.; Zellner, R. *Phys. Chem. Chem. Phys.* **2000**, *2*, 1899–1905.
(49) Dybala-Defratyka, A.; Paneth, P.; Pu, J.; Trular, D. G. *J. Phys. Chem. A* **2004**, *108*, 2475–2486.
(50) Lendvay, G.; Viskolcz, B. *J. Phys. Chem. A* **1998**, *102*, 10777–10786.
(51) Zhang, Y.; Zhang, S. W.; Li, Q. S. *Chem. Phys.* **2005**, *308*, 109–116.
(52) Hoyermann, K.; Olzmann, M.; Seeba, J.; Viskolcz, B. *J. Phys. Chem. A* **1999**, *103*, 5692–5698.
(53) Hallquist, M.; et al. *Atmos. Chem. Phys.* **2009**, *9*, 5155–5236.
(54) Caralp, F.; Devolder, P.; Fittschen, C.; Gomez, N.; Hippler, H.; Mereau, R.; Rayez, M. T.; Striebel, F.; Viskolcz, B. *Phys. Chem. Chem. Phys.* **1999**, *1*, 2935–2944.
(55) Zhang, Y.; Zhang, S. W.; Li, Q. S. *Chem. Phys.* **2004**, *296*, 79–86.